Singularities in Scattering of Atomic Particles in Collisions Involving the Excitation of Inner Electron Shells

V. V. AFROSIMOV, YU. S. GORDEEV, V. K. NIKULIN, A. M. POLYANSKIĬ, AND A. P. SHERGIN

A. F. Ioffe Physico-technical Institute, USSR Academy of Sciences

Submitted August 23, 1971

Zh. Eksp. Teor. Fiz. **62**, 848–862 (March, 1972)

Scattering of atomic particles with energies of 10–180 keV has been studied in the range of distances of closest approach at which the inner electron shells cross. In collisions of N^+, Ne^+, Ar^+, Kr^+, and Xe^+ ions with atoms of Ne, Ar, Kr, and Xe, structure (singularities) was observed in the differential scattering cross sections. High total angular resolution of $7.5' \pm 0.5'$ and accuracy of ~ 0.5% permitted studying the location and shape of the singularities. A correlation has been established between the scattering singularities and formation of vacancies in internal shells, which permits the singularities to be interpreted as the result of the multichannel nature of scattering. A simplified description of a collision is proposed, in which there are two effective terms—a ground term corresponding to excitation only of outer electron shells, and an excited term corresponding to additional excitation of internal shells. The deflection angle and differential scattering cross section have been calculated for each of the possible channels in the classical and quasiclassical approximations. The theoretical cross sections have peaks which agree qualitatively with the experimentally observed scattering singularities. The effective interaction potentials have been determined from the experimental scattering cross sections by the Firsov Method.

1. INTRODUCTION

IN previous work[1] we have studied the scattering of atomic particles for distances of closest approach much smaller than the atomic dimensions. The total flux of particles scattered by a given angle ϑ was measured, independently of their final charge state. It was observed that the scattering cross section at such approach distances is not a monotonic function of the scattering angle as had been assumed earlier. At some angles singularities were observed in the scattering cross sections. The singularities had the form of peaks superposed on differential cross sections falling off smoothly with increasing scattering angle

$$\sigma'(\vartheta) \equiv \frac{d\sigma}{d\omega}(\vartheta).$$

Subsequently Loftager and Claussen[2] also observed singularities in scattering for deep collisions.

The present work is devoted to study of the properties of the singularities in scattering cross sections and to discussion of the interaction mechanism leading to these singularities. An initial report of the results obtained was given at the 1971 ICPEAC.[3] Scattering of He^+, N^+, Ne^+, Ar^+, Kr^+, and Xe^+ ions by atoms of Ne, Ar, Kr, and Xe was studied for incident-particle energies of 10—180 keV and scattering angles of 3—43°.

2. EXPERIMENTAL METHOD

The measurements were made in a modified version of the apparatus described previously,[4] and part of them in the apparatus described by Kaminker and Fedorenko[5], which was rebuilt to measure differential scattering cross sections over a wide range of the angle ϑ. Ions from a source were accelerated to a given energy T_0 and sorted in m/e by means of a magnetic mass monochromator. The divergence of the primary beam was reduced to 5′. The narrow beam of ions entered the collision chamber and was scattered by a gas target. The gas pressure in the collision chamber was chosen from the condition of single collisions and was $\sim 4 \times 10^{-4}$ mm Hg. Particles scattered by a given angle ϑ were separated by a collimator with a divergence of 5.1′ and were recorded by a detector working in the individual-particle counting mode.

The total angular resolution of the apparatus (the width of the instrumental response function at half-height) due to the horizontal and vertical divergence of the primary beam and the scattered-particle beam was $7.5' \pm 0.5'$. This permitted observation of singularities in all cases studied and study of the shape of the singularities, since it was known from our earlier work[1] that the width of the singularities was several degrees.

In order to monitor the constancy of the primary ion-beam intensity and the gas pressure in the collision chamber during measurement of the angular dependence $\sigma'(\vartheta)$, a second scattered-particle collimator was used, which was set a fixed angle φ to the primary beam direction. The statistical error determined by the number of counts was reduced to ~0.5%.

A number of factors were considered which could result in distortion of the location and shape of the singularities: existence of several isotopes and thermal motion of the gas-target atoms, and also instability in the accelerating voltage. The errors in determination of the location and shape of the singularity resulting from these factors for the case of a Kr target were respectively 6′, 5′, and 3′ for a scattering angle $\vartheta = 10°$. The effect of the residual magnetic field inside the apparatus and of the energy spread of the ions in the source leads to uncertainties in the location and shape of the singularities of 0.2′ and 0.3′. The total error in measurement of the position and shape of a singularity resulting from all the factors enumerated does not exceed ±8.5′.

A number of control experiments were made before measurement of $\sigma'(\vartheta)$. In order to determine the reference zero of the scattering angle, the primary beam current I_0 was measured as a function of ϑ. The value $\vartheta = 0$ was established from the maximum value

of I_0. The accuracy in determination of $\vartheta = 0$ was ~1′.

Before study of each pair of colliding particles, the purity of the target-gas was checked. Here the gas was fed into the collision chamber and ionized by the primary beam. The ions produced were extracted by an electric field and analyzed for m/e in the magnetic field by means of a mass spectrometer connected to the chamber.

For correct measurement of the scattering cross sections and, consequently, the shape of the singularities, it is important to know the detection efficiency for particles of different charges. This is due to the fact that in the range of T_0 and ϑ studied the charge composition of the scattered particles changes very rapidly with T_0 and ϑ. In measurement of the total flux of scattered particles as a function of angle ϑ, the individual-particle counting method was used. Before detection, all charged particles were accelerated by a fixed voltage of ~15 kV and thus acquired different energies. To measure the efficiency, a particle beam of definite charge was separated and the beam current was compared with the counting rate of pulses in the counting equipment. Conditions were provided under which the detection efficiency for charged particles with different initial energies and charges was close to 100%.

The background due to scattering in the residual gas was small (of the order of a few per cent of the scattering in the gas being studied) in scattering of heavy primary ions and turned out to be large (~tens of per cent) in scattering of He^+ ions.

3. RESULTS

In the range of collision energy T_0 and scattering angle ϑ studied, the incident-particle wavelength is much smaller than the characteristic size of the interaction region $\sim a_0$, and the scattering angle is $\vartheta \geq 3°$, which is much greater than the minimal deflection angle determined by the uncertainty relation. In this case the particle motion can be considered classical and characterized by an impact parameter ρ and distance of closest approach r_0.

Strictly speaking, the collisions being considered are inelastic. The ratio of the inelastic energy loss Q to the incident-particle kinetic energy T_0, as follows from the experimental data[6-10], is small and amounts to ~1–2%. Therefore trajectory of the inelastically scattered particle should not differ in any important way from the trajectory of an elastic scattering. In the present work we have compared the classical elastic-scattering cross sections calculated by us for the Bohr[11], Thomas-Fermi, and Thómas-Fermi-Dirac[12,13] potentials, employing quantum-mechanical electron density distributions in the atoms, with the measured cross sections. The latter two calculations are in good agreement with each other and describe the greater part of the measured cross sections better than the calculation with the Bohr[11] potential. An example of comparison of the measured cross section with that calculated from the Thomas-Fermi potential[12] is given in Fig. 1. It is evident that the real interaction differs from the interaction described by the statistical model, but the extent of deviation of the experimental

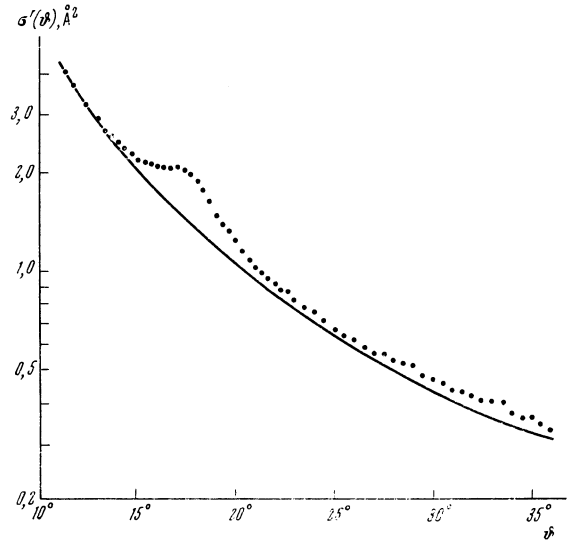

FIG. 1. Differential scattering cross section $\sigma' \equiv d\sigma/d\omega$ as a function of scattering angle ϑ for Kr^+–Kr collisions, T_0 = 12.5 keV. Points–experimental data of the present work, curve–theoretical calculation with a Thomas–Fermi potential. [12] The cross section and angle are in the laboratory system.

cross sections outside the singularities from the calculated values is small and in most cases does not exceed 20–30% in the angular region $\vartheta > 40°$. This permits us to use the classical scattering calculations for evaluation of the collision parameters.

A. Properties of the Singularities

In order to analyze the shape of a singularity, we took into account the monotonic part of the scattering cross section $\sigma'(\vartheta)$. Here the measured cross section was matched with the calculated value[12] at a point $\vartheta = 4°$ and the ratio $\sigma'_e(\vartheta)/\sigma'_t(\vartheta)$ was calculated. The function obtained in this way is shown in Fig. 2. The location of a singularity ϑ^* was determined from the maximum deviation of the experimental cross section from the monotonic component $\sigma'(\vartheta)$, the width of the singularity $\Delta\vartheta^*$ from the width of the function $\sigma'_e(\vartheta)/\sigma'_t(\vartheta)$ at half-height, and the amplitude of the singularity h from the value of the ratio $\sigma'_e(\vartheta^*)/\sigma'_t(\vartheta^*)$ at the peak of the distribution.

The singularity parameters obtained in this way are given in the table.

Measurements of the singularities for each pair of colliding particles for several incident-particle energy values T_0 showed that the singularity location ϑ^* and width $\Delta\vartheta^*$ change with energy T_0 in such a way that the products $T_0\vartheta^*$ and $T_0\Delta\vartheta^*$ remain constant. In classical scattering of particles of different energies in the same potential V(r), in the small-angle approximation a fixed value of $T_0\vartheta$ corresponds to a definite distance of closest approach r_0. Thus, appearance of a singularity corresponds to approach of the particles to a definite distance r_0^*.

It should be noted that variation of T_0 permits the singularities studied by us to be distinguished from peaks of some other kind, for example, the peak corresponding to a limiting scattering angle which arises in scattering of a heavy particle by a light particle and

Pair	T_0, keV	ϑ^*, deg	$\Delta\vartheta^*$, deg	r_0^*, Å	δ	h	Interacting shells	ρ(r)
Ar^+—Ar	25	14.2	5.6	0.28	0.13	1.35	L_{Ar}—L_{Ar}	21—21
	50	6.3	3	0.28	0.13	1.45	»	21—21
	50[2]	7	4	0.28	0.13	1.40	»	21—21
Kr^+—Kr	12.5	17.6	4	0.52	0.11	1.45	M_{Kr}—M_{Kr}	38—38
	18[2]	12.5	—	0.52	0.11	1.55	»	38—38
	25	8.8	2.2	0.52	0.11	1.70	»	38—38
	50	4.4	1	0.52	0.11	1.60	»	38—38
	180	9.4	2.5	0.23	0.28	1.30	M_{Kr}—L_{Kr}	38—54
	180	21	15	0.15	0.11	1.20	L_{Kr}—L_{Kr}	54—54
	300[2]	5.4	—	0.23	0.28	1.30	M_{Kr}—L_{Kr}	38—54
Xe^+—Xe	12.5	10	5	0.77	0.10	1.15	N_{Xe}—N_{Xe}	27—27
	25	22	10	0.50	0.14	1.20	N_{Xe}—M_{Xe}	27—77
	50	11	5.5	0.50	0.14	1.20	»	27—77
	165	18.5	7	0.25	0.22	1.15	M_{Xe}—M_{Xe}	77—77
Kr^+—Xe	50	17.5	6	0.30	0.17	1.20	M_{Kr}—M_{Xe}	38—77
N^+—Kr	12.5	20	11	0.28	0.10	1.15	K_N—M_{Kr}	73—38
Ne^+—Kr	40	12.4	3	0.23	0.18	1.12	K_{Ne}—M_{Kr}	108—38
Ar^+—Kr	12.5	20	9	0.44	0.15	1.23	L_{Ar}—M_{Kr}	21—38
	25	10	5	0.44	0.15	1.20	»	21—38
	50	5	3	0.44	0.15	1.30	»	21—38

Here T_0 and ϑ^* are the energy and angle in the laboratory system, r_0 is the distance of closest approach [12], $\delta = (R_i + R_j - r_0)/(R_i + R_j)$ is the degree of overlap of the electron shells, R_i and R_j are the radii of the interacting shells, $\rho(r)$ [14] is the "linear" electron density in the radial direction in units of $1/\alpha_0$.

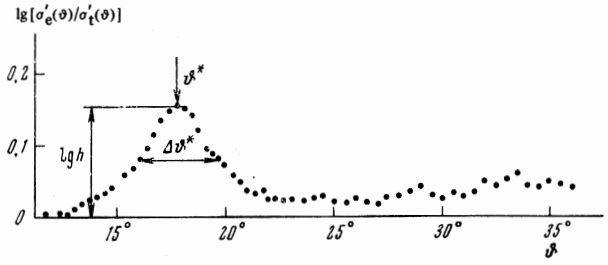

FIG. 2. Scattering singularity for Kr^+-Kr, T_0 = 12.5 keV. ϑ^* = 18° is the location of the singularity, $\Delta\vartheta^*$ = 4° is the width of the singularity, h = 1.5 is the amplitude of the singularity.

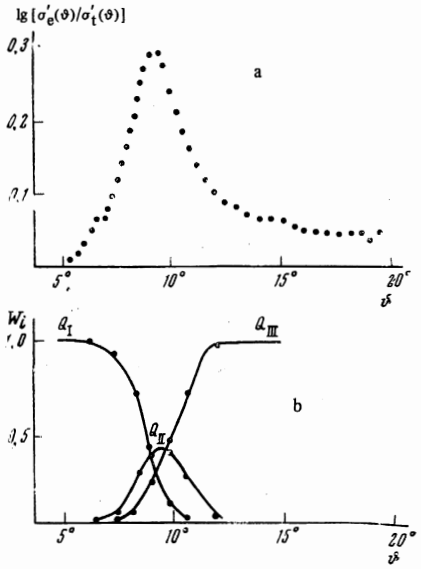

FIG. 3. a—Scattering singularity for Kr^+-Kr; T_0 = 25 keV, ϑ^* = 8.8°, $\Delta\vartheta^*$ = 2.2°, h = 1.7. The singularity location ϑ^* corresponds to r_0^* = 0.52Å, [12] which corresponds to crossing of the M shells of Kr. b—Probabilities W_i for excitation of various lines of discrete energy loss as a function of scattering angle ϑ for Kr^+-Kr collisions, T_0 = 25 keV. [7] Q_I = 76 ± 6 eV—excitation of outer shells, Q_{II} = 167 ± 6 eV—further removal of one M electron, Q_{III} = 255 ± 8 eV—further removal of two M electrons.

whose position ϑ_{lim} is determined only by the mass ratio of the partners and does not depend on the collision energy.

The distances r_0^* found in the present work, corresponding to appearance of singularities, were compared with the sizes of the atomic electron shells. As the size of an electron shell we chose the distance from the center of the atom to the position of the maximal electron density of this shell. Electron density data obtained from quantum-mechanical calculations[14] were used. It turned out that as r_0 is decreased in scattering, singularities arise when new, deeper shells intersect, and the maximum of the singularity corresponds to a certain degree of overlap of these shells δ (see the table). The quantity δ is defined as

$$\delta = (R_i + R_j - r_0^*) / (R_i + R_j),$$

where R_i and R_j are the radii of the interacting shells. Knowing the radii of the electron shells[14] and the degree of overlap δ, which in the cases studied amounted to 0.1—0.3, we could predict the singularity location r_0^* for pairs of colliding particles not yet studied.

B. Singularities and Inelastic Energy Loss

It is well known that in achieving collision distances corresponding to intersection of internal shells, strong excitation and ionization of the atoms occurs. Here the spectrum of inelastic energy loss consists of several discrete lines. Thus, in our studies[6,7,10] and in those of other workers[8,9] it has been shown that deep collisions with participation of Ne, Ar, Kr, and Xe are accompanied by appearance of discrete lines in the inelastic energy-loss spectrum. The lowest-energy line is due to excitation of outer shell electrons. Each of the higher lines is associated with additional excitation of individual electrons of inner shells.

In Fig. 3 we have compared the location of a singularity obtained in the present work with the dependence

of the relative probabilities W_i for excitation of various lines Q_I, Q_{II}, and Q_{III} on the angle ϑ, obtained by us[7] for Kr^+-Kr collisions for $T_0 = 25$ keV. It is evident that the singularity appears at angles corresponding to formation of vacancies in the M shell of Kr (the lines Q_{II} and Q_{III}). Similar comparisons have been made for $Ar^+ - Ar$, $Ne^+ - Ar$, and $Xe^+ - Xe$ collisions. Thus, the singularities are observed at the same closest approach distances at which a sharp change is observed in the probabilities for excitation of the various lines in the inelastic energy-loss spectrum.

4. DISCUSSION

A. Description of Scattering by Means of a System of Crossing Terms

The comparisons made in the present work of the location of a singularity with inelastic transitions in deep collisions permits the scattering singularities to be interpreted as the result of excitation of inner-shell electrons. Knowing the mechanism of inner-shell excitation, we can attempt to describe the particle scattering which leads to appearance of the singularities.

In experimental studies of inelastic energy loss[6-10] the conclusion has been drawn that excitation of inner shells is due to vacancy formation. The vacancy-formation mechanism is distinct from an impact mechanism, since in the incident-particle energy range studied the collisions are "slow" (the velocities of the relative motion of the atomic particles v_0 are substantially smaller than the velocities of the internal electrons). For example, in $Ar^+ - Ar$ collisions with $T_0 = 50$ keV, the velocity v_0 is 0.5×10^8 cm/sec, and $v_{LII,III} = 9.5 \times 10^8$ cm/sec, i.e., $v_0 \ll v_L$.

As can be seen from Fig. 3, excitation of internal shells (the lines Q_{II} and Q_{III}) has a threshold nature and begins when a definite distance between the particles is reached. Study of the excitation probabilities of various energy-loss lines as a function of incident-particle initial energy in ref. 1 for $Ar^+ - Ar$ collisions and in the present work for $Kr^+ - Kr$ collisions at $T_0 = 12.5$ and 25 keV indicates that the excitation probabilities of various lines depend only weakly on velocity and are determined mainly by the distance between the particles.

Existence of a characteristic distance which does not depend on velocity is inherent in processes which can be described by crossing terms. Here the formation of internal vacancies can be considered as the result of transitions on crossing of a term corresponding to a state with internal vacancies by terms of lower-lying states. The experimentally observed characteristic distance can be considered in the first approximation as the coordinate of the point of crossing of the terms. Thus, we can attempt to explain scattering singularities in deep collisions by formation of vacancies in the inner shells on crossing of the terms of the quasimolecule.

As a result of the complexity of exact quantum-mechanical calculation of such a system of terms, at the present time terms have been calculated only for the simplest cases of the type H – H, He – He, $He^+ - H$.[15] In order to describe deep collisions of complex atoms it is necessary to use approximate means of constructing the pattern of term crossing. Thus, qualitative agreement with the data on internal vacancy formation is given by the model of Fano and Lichten.[16]

Formation of $L_{II,III}$ vacancies in Ar and of $M_{IV,V}$ vacancies in Kr is explained by the advance of the molecular term $4f\sigma$ formed from the 2p-electron terms of Ar, or of the terms $5g\sigma$ and $6h\sigma$ formed from the 3d-electron terms of Kr, and crossing of these terms by upper unfilled terms. However, in spite of the fact that it is possible in a number of cases to identify the initial state of the electron removed from the inner shell, the exact term of the quasimolecule remains uncertain. This is due to the fact that, in deep collisions of complex atoms, excitation of inner shells always occurs in a background of outer-shell excitation due to a large number of transitions. As a result, discussion of transitions of inner-shell electrons is possible only by methods which permit substantial simplification of the problem.

As has been shown by us and by other workers[6-10] the spectra of inelastic energy loss consist of well resolved lines corresponding to excitation of different shells. Therefore as a first approximation we can neglect the change in energy of the system as the result of transitions of inner-shell electrons to different final states and consider only the energy changes associated with transitions of various numbers of such electrons. Thus, a system of a large number of quasimolecule terms is replaced by a rather simple system of several effective terms.

B. Calculation of Scattering in the Two-term Approximation

In the present work we have identified two effective terms. Each term is characterized by a certain average configuration of electron states of individual shells, from which transition of electrons occur to other states or to the continuum.

From the experiments described by us previously[6] it is known that in excitation of outer shells, in the region of closest approach distances corresponding to a scattering singularity, each particle loses on the average two M electrons. Therefore as a ground-state term which describes scattering with excitation only of outer electrons we chose a term corresponding to infinite distance between particles of a doubly charged Ar^{2+} ion, i.e., $3p^4$. Scattering with excitation of both outer and inner shells was described by means of an excited term corresponding to additional formation of two $L_{II,III}$ vacancies—one in each of the particles, i.e., to an ion configuration $2p^5 3s^2 3p^4$. As was established by us previously,[10] the two L vacancies can be formed in one particle with an appreciable probability, i.e., the term corresponding to ion states $2p^6 3s^2 3p^4$ and $2p^4 3s^2 3p^4$ can also be considered as an excited term. Calculations show that the terms of these two configurations are practically the same.

The terms were calculated in the framework of the statistical model of the atom with use of quantum-mechanical electron densities. The details of similar calculations are presented by Nikulin.[13] The terms

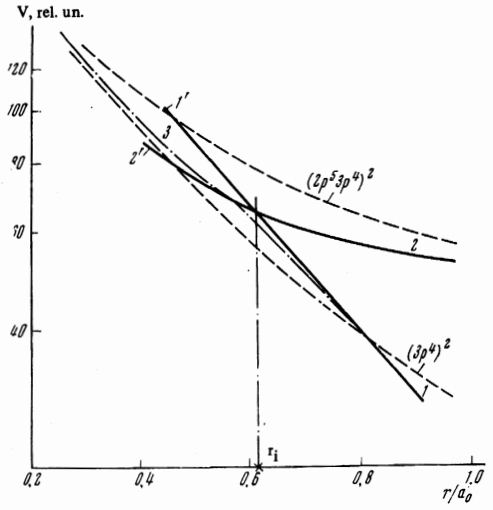

FIG. 4. Terms of the Ar^+–Ar system. Dashed line–adiabatic terms for electron-shell configurations arbitrarily designated $(3p^4)^2$ (ground-state) and $(2p^5 3p^4)^2$ (excited-state). Solid lines–diabatic terms of the ground (1, 1′) and excited (2, 2′) states. The terms have the form $V(r) = Ar^{-1}e^{-\alpha r} + V_0$; r_c is the point of crossing of the terms corresponding to the onset of internal vacancy formation. Curve 3 is the potential reproduced from the experimental data by the Firsov method. [17]

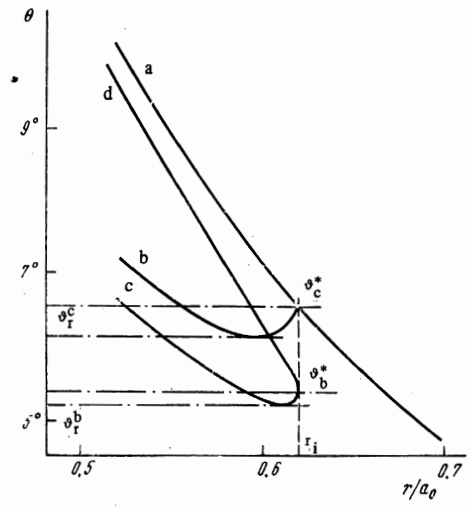

FIG. 5. Deflection angle θ as a function of r for the processes (see Fig. 4): a–1-1′-1, b–1-2′-1, c–1-2′-2, d–1-1′-2. Here ϑ_r^b and ϑ_r^c are the rainbow angles for processes b and c; ϑ_b^* and ϑ_c^* are the boundary of the multiple-valued function $\theta(r)$.

calculated in this way describe elastic scattering of particles in various states with "frozen" electron-density distributions in the shells and are called adiabatic.

Our adiabatic terms of the ground and excited states nowhere cross. Real scattering is accompanied by inelastic transitions (successive radiation of the lines Q_{II} and Q_{III}; see Fig. 3b). Transitions between states can be described by means of diabatic effective terms which cross. The diabatic terms were constructed so that their point of crossing corresponded to the experimentally measured threshold for excitation of inner-shell electrons. The purpose of the calculation was to study qualitatively the main properties of a description of scattering by means of a system of diabatic terms. Therefore the angle between the terms at the point of crossing was chosen to be large, since in this case the interaction force changes more sharply, and effects in the scattering associated with occurrence of transitions are amplified. Terms of the system $Ar^+ - Ar$ calculated in this way are shown in Fig. 4.

In the model used, scattering occurs as follows. At large distances the system converges along the ground-state term 11′. Transitions occur at the point r_c. Up to the turning point the system can converge along two trajectories 1′ and 2′. Separation is possible both along the ground-state term 1—the quasielastic channel, and along the excited-state term 2—the inelastic channel, which are experimentally distinguished by the inelastic energy loss.

For each of the four possible processes the classical deflection angle $\theta_a - \theta_d$ was calculated with use of the specified diabatic terms. The results of the calculation are shown in Fig. 5. It is evident that purely elastic scattering along term 11′ corresponds to a monotonic dependence of the deflection angle on the internuclear distance (curve a in Fig. 5).

In the case in which a transition occurs to an excited-state term in the convergence process, the dependence of the deflection angle on distance becomes more complicated. Thus, for processes b and c (Fig. 5) the function $\theta_i(r)$ has a minimum. The minimum in the deflection angle as a function of distance is due to the fact that a transition to the term 22′ on traversal of the crossing point r_c in the convergence process is accompanied by a sharp decrease in the repulsive force between the atoms (an effective attraction). Since the main contribution to $\theta_i(r)$ in the integration is from the region close to the classical turning point r_0, a decrease in the interaction force in the region $r_c - r_0$ leads to a significant reduction in the deflection angle in this range of distances.

Thus, the calculation carried out of the deflection angle $\theta_i(r)$ for the various processes a–d permits us to draw the important conclusion that the classical deflection angle can have a minimum in scattering by a monotonic repulsive potential with a break (the first derivative undergoes a discontinuity). As far as we know, this fact was noted for the first time by Marchi[18] in analysis of the oscillations of the elastic-scattering cross section at large internuclear distances.

From the deflection functions obtained, the classical scattering cross sections were calculated for each of the processes considered. Elastic scattering along the ground-state term corresponds to the cross section for process a (Fig. 6). Existence of a minimum in the classical deflection function for processes b and c leads, as in the case of an attractive scattering potential, to appearance of a singularity in the classical differential scattering cross section at respective angles ϑ_r^b and ϑ_r^c (Figs. 5 and 6). By analogy with the cross-section maxima observed in scattering by a potential with a minimum for large intranuclear distances—the so-called rainbow scattering, the maxima in the case of scattering by a purely repulsive potential can also be considered as a rainbow effect.[19]

The total differential scattering cross section can be obtained by summing the partial cross sections for processes a–d multiplied by the probabilities of these

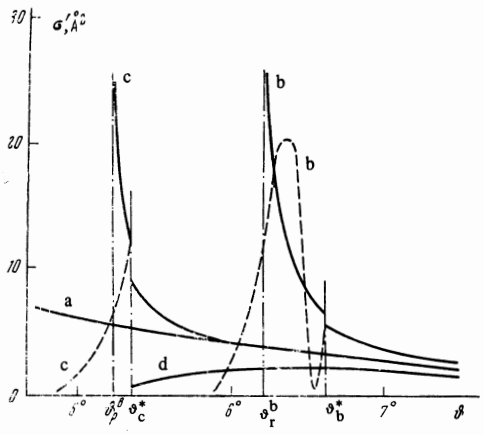

FIG. 6. The function $\sigma_i'(\vartheta)$ for processes a–d (Fig. 5); solid lines–theory in the classical approximation, dashed lines–in the quasiclassical approximation. ϑ_r^b and ϑ_r^c are the rainbow angles; ϑ_b^* and ϑ_c^* are the boundary of the multiple-valued function $\theta(r)$.

processes. It is evident from Fig. 6 that, like the experimental cross section, before and after a singularity the calculated cross sections are a smooth function of the angle ϑ. In the vicinity of a singularity, maxima appear in the cross sections for processes b and c.

As is well known, in those cases in which the variation of the force in a distance equal to the wavlength of the scattered particle is small, the quantum-mechanical description of scattering coincides with the classical description. In the transition to another term, the interaction force changes discontinuously practically at the point r_c. In addition, in the region $r < r_c$ two trajectories are possible which are indistinguishable. Therefore for completeness of description of the scattering pattern it is necessary to take into account the wave properties of the particles. For this purpose a calculation of the scattering near the crossing point and to the left of it has been made in the quasiclassical approximation.

We will consider three regions of deflection angle:

1. The region $\vartheta < \vartheta_r$ (Fig. 5); here the classical calculation agrees with the quasiclassical (cross section a in Fig. 6).

2. The region $\vartheta > \vartheta_{b,c}^*$ (Fig. 5); the contribution to the cross section for quasielastic ($\sigma_{q\text{-}e}'$) and inelastic (σ_{in}') scattering is due to two trajectories (a, b for quasielastic and c, d for inelastic). In the Landau-Zener-Stueckelberg model[20,21] these cross sections have the following form:

$$\sigma_{q\text{-}e}'(\vartheta) = (1-P)_b^2\sigma_b'(\vartheta) + P_a^2\sigma_a'(\vartheta) + 2(1-P)_b^2P_a[\sigma_b'(\vartheta)\sigma_a'(\vartheta)]^{1/2}\cos(\alpha_a-\alpha_b), \quad (1)$$

$$\sigma_{in}'(\vartheta) = (k/k_1)\{[P(1-P)]_d\sigma_d'(\vartheta) + [P(1-P)]_c\sigma_c'(\vartheta) - 2[P(1-P)]_d^{1/2}[P(1-P)]_c^{1/2}[\sigma_d'(\vartheta)\sigma_c'(\vartheta)]^{1/2}\cos(\alpha_c-\alpha_d)\}.$$

Here $P_i(T_0, r_0)$ is the transition probability from a ground-state adiabatic term to an excited-state term, i.e., the probability that the system will remain in the ground-state diabatic term for a single passage through the crossing point r_c; α_i are phase angles, k and k_i are wave numbers before and after the collision, which differ insignificantly. In the Landau-Zener model the probability $P_i(T_0, r_0)$ is calculated at the point r_c; before reaching the crossing point it is assumed to be unity.

It can be seen from Fig. 5 that for $\vartheta > \vartheta_b^*$ the deflection angles for processes b and c are close to those of processes a and d. We can therefore assume that $\sigma_a'(\vartheta) \approx \sigma_d'(\vartheta)$ and $\sigma_b'(\vartheta) \approx \sigma_c'(\vartheta)$, $\alpha_a - \alpha_d \approx \alpha_b - \alpha_d$ (Fig. 6), and also the values of $P_i(T_0, r_0)$ are close. This leads to a mutual compensation of the interference terms in the total cross section, and for large angles it reduces to the more simple form:

$$\sigma_{q\text{-}e}'(\vartheta) + \sigma_{in}'(\vartheta) = [P\sigma'(\vartheta)]_d + [(1-P)\sigma'(\vartheta)]_b. \quad (2)$$

The result obtained has a simple physical interpretation: scattering in this angular region can be described as scattering by adiabatic potentials of the ground and excited states.

3. The region $\vartheta_r^b < \vartheta < \vartheta_b^*$ (Fig. 5). In the region of the minimum of the function $\theta_b(r_0)$ the quasielastic-scattering cross section in the quasiclassical approximation can easily be obtained by following the well known procedure of Ford and Wheeler.[22] In place of $\sigma_b'(\vartheta)$ it is necessary to substitute only $I_r^b(\vartheta)$:

$$I_r^b(\vartheta) = 2\pi\frac{\rho_r q^{-2/3}}{k\sin\vartheta}\mathrm{Ai}^2(x), \quad x = q^{-1/3}(\vartheta_r - \vartheta), \quad q = \frac{1}{2k^2}\left(\frac{d^2\theta}{d\rho^2}\right)_{\rho_r}, \quad (3)$$

where the values of ϑ_r, ρ_r, and θ should be marked with an index b: Ai(x) is the Airy function.

Similar calculations can be carried out for rainbow scattering in the inelastic channel. For $\vartheta_r^c < \vartheta < \vartheta_c^*$ we have

$$\sigma_{in}'(\vartheta) = (k/k_1)[P(1-P)I_r(\vartheta)]_c, \quad (4)$$

where $I_r^c(\vartheta)$ is given by Eq. (3) (with ϑ_r, ρ_r and θ marked with the process index c).[1)] The scattering cross sections in the vicinity of the rainbow angles for processes b and c are shown by the dashed curves in Fig. 6a.

Thus, in the description presented of the form of the partial cross sections for scattering at various angles ϑ, two types of interference are present:

a) in the large-angle region $\vartheta > \vartheta_{b,c}^*$ interference is present in the quasielastic and inelastic channels as the result of the two possible trajectories to the left of the crossing point r_c. It has been shown that in the total cross section for sufficiently large values of ϑ the interference contributions in the two channels are mutually compensated, since the values of $\sigma'(\vartheta)$ are close (see Fig. 6, $\vartheta > \vartheta_b^*$) and the channels are supplementary with respect to each other;

b) there is interference in the quasielastic and inelastic channels associated with the multiple value of the function $\theta(r)$ in the range $\vartheta_r^{b,c} < \vartheta < \vartheta_{b,c}^*$ (the fine structure of the rainbow in Fig. 6). Since the effective term is in fact the averaged description of a group of states, in transition to a real situation observable in experiment this can lead to a redrawing of the remaining interference pattern in the total cross

[1)]Expressions which are a special case of Eqs. (1), (3), and (4) in the rainbow-scattering region have been obtained, as we have recently learned, by Kotova and Ovchinnikova.[23] The formulas given by those authors can be derived from (1), (3), and (4) by expansion of the transition probability in a series in the interaction and by use of the first order of the expansion (see also the review of Nikitin and Ovchinnikova[24]).

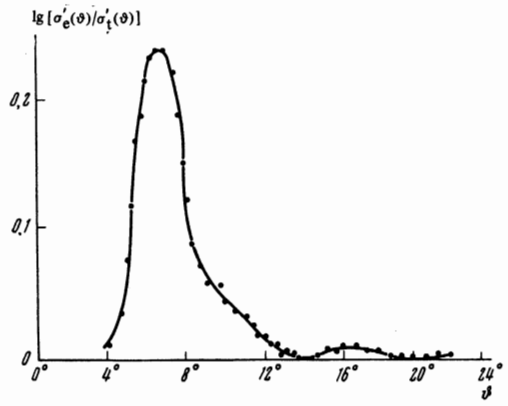

FIG. 7. Scattering singularity obtained in Ar^+–Ar scattering, T_0 = 50 keV; $\vartheta^* = 6.3°$, $\Delta\vartheta^* = 3°$, h = 1.45.

section as the result of contributions from many crossings within the effective width of the term. In the angular region $\vartheta < \vartheta_r$ and $\vartheta > \vartheta^*$ the cross sections $\sigma'_{q\text{-}cl}(\vartheta) \approx \sigma'_{cl}(\vartheta)$, and for $\vartheta_r < \vartheta < \vartheta^*$ the singularity in the scattering cross section will be represented by the main rainbow maximum of the quasiclassical calculation (Fig. 6). It should be noted that the depth of the minimum for θ_b and θ_c, and consequently also the amplitude and width of the rainbow maximum, depend substantially on the angle between the crossing terms.

Returning to comparison of the theoretical cross sections with the experimentally observed singularity in Fig. 7, we can note that in the measured cross section there is no structure associated with the rainbow maxima of processes b and c. This is explained by the fact that within the effective width of the term there actually occur not one but several crossings of the terms. As a result a superposition occurs of the maxima from each crossing and formation of a single broad distribution as in Fig. 7.

Thus, the analysis of the experimental data and the scattering calculation carried out in the two-term approximation qualitatively explain the origin of singularities in scattering. The quantitative characteristics of the effective terms of the quasimolecule can be obtained on comparison of the theoretical calculation with data on scattering and inelastic energy loss. At the present time the quasimolecule terms have been successfully reproduced[25-27] for large internuclear distances at which it is possible to separate individual electronic transitions.

The model considered permits in principle the description of a scattering singularity by means of a system of purely repulsive terms. It is necessary to keep in mind that real effective terms may differ from those which we have discussed. Possible corrections to the terms which we have discussed include more accurate allowance in the calculation for exchange and polarization interaction terms which are superposed on the strong repulsion (the repulsion in the region of the singularity for Kr^+ – Kr is ~1.5 keV) and should partially compensate it. For deep collisions leading to formation of a singularity, the conditions are realized which are necessary for appearance of significant exchange forces: the inner shells overlap and cease to be closed in the quasimolecule, as the result of formation in them of vacancies. In regard to the polarization interaction, it should not be small, since after traversal of the outer shells the subsequent approach of the atomic cores will occur in the field of Coulomb charges $+Z_n e$, where Z_n is the charge of the outer shell.

C. Description of Scattering by Means of an Effective Interaction Potential

From the comparison shown in Figs. 6 and 7, it is evident that in measurement of the total differential scattering cross sections (Fig. 7) we automatically average all multichannel scattering cross sections which contribute to the total cross section. If we reproduce the interaction potential from the total differential cross section, assuming elastic scattering, it will carry information on the average value of the forces acting between the particles during the collision, i.e., such a potential can be considered as effective with respect to the scattering pattern described by the system of terms.

From our data on scattering, the effective potential can be obtained by the method proposed by Firsov.[17] The method establishes a relation between the interaction potential V(r) and the measured dependence $\sigma'(\vartheta)$. The potential obtained in this way for Ar^+ – Ar collisions at T_0 = 50 keV is shown in Fig. 4 (curve 3). It can be seen that the effective potential is in reasonable agreement with the diabatic terms 11′ and 22′. Up to the crossing point r_c where the excitation probability of inner shells is small, the effective potential 3 is close to the ground-state term 11′, and for small r, where the role of internal-shell excitation becomes important, the effective potential passes between the ground-state (1′) and excited-state (2′) terms. In the region of distances of closest approach corresponding to appearance of a singularity, a change in the slope of the potential is observed.

Similar curves for $V_{eff}(r)$ have been obtained for Kr^+ – Kr collisions at T_0 = 12.5, 25, and 50 keV. On comparison of the potentials calculated for the different energies, a weak dependence of these potentials on velocity is observed. For T_0 = 12.5 keV, scattering in the quasielastic channel is dominent, and for T_0 = 50 keV, scattering occurs in the inelastic channel with a higher probability than for 12.5 keV. A change in the slope of the potential is observed in the vicinity of the singularity in all three cases.

Thus, although the effective interaction potentials depend on velocity, this dependence is small in the energy region studied, and therefore the effective potential can be fully used to describe the scattered-particle angular distribution pattern.

In conclusion the authors express their gratitude to N. V. Fedorenko for his constant interest in this work, and to Yu. N. Demkov and M. Ya. Ovchinnikova for helpful discussion of the results.

[1]V. V. Afrosimov, Yu. S. Gordeev, N. M. Panov, and N. V. Fedorenko, Zh. Tekh. Fiz. **36**, 123 (1966) [Sov. Phys. Tech. Phys. **11**, 89 (1966)]; V. V. Afrosimov, Yu. S. Gordeev, A. M. Polyansky, and A. P. Shergin, V ICPEAC, (International Conference on Physics of Electronic and Atomic Collisions) Abstracts of papers, Nauka, Leningrad, 1967, p. 475.

[2]P. Loftager and G. Claussen, VI ICPEAC, Abstr. of papers, MIT Press, Cambridge, 1969, p. 518.

[3]V. V. Afrosimov, Yu. S. Gordeev, V. K. Nikulin, A. M. Polyansky, and A. P. Shergin, VII ICPEAC, Abstr. of papers, Amsterdam, The Netherlands, 1971, p. 149.

[4]V. V. Afrosimov, Yu. S. Gordeev, M. N. Panov, and N. V. Fedorenko, Zh. Tekh. Fiz. **34,** 1613 (1964) [Sov. Phys. Tech. Phys. **9,** 1248 (1965)].

[5]D. M. Kaminker and N. V. Fedorenko, Zh. Tekh. Fiz. **25,** 1843 (1955).

[6]V. V. Afrosimov, Yu. S. Gordeev, M. N. Panov, and N. V. Fedorenko, Zh. Tekh. Fiz. **34,** 1624 (1964) [Sov. Phys. Tech. Phys. **9,** 1256 (1965)]; V. V. Afrosimov, Yu. S. Gordeev, A. M. Polyanskiĭ, and A. P. Shergin, Zh. Eksp. Teor. Fiz. **57,** 806 (1969) [Sov. Phys. JETP **30,** 441 (1970)].

[7]V. V. Afrosimov, Yu. S. Gordeev, A. M. Polyanskiĭ, and A. P. Shergin, Zh. Tekh. Fiz. **42** (1), ,(1972) [Sov. Phys. Tech. Phys. **17** (1), ,(1972) (in press)].

[8]Q. C. Kessel, M. P. McCaughey, and E. Everhart, Phys. Rev. **153,** 57 (1967).

[9]B. Fastrup and G. Herman, Phys. Rev. Lett. **23,** 157 (1969).

[10]V. V. Afrosimov, Yu. S. Gordeev, A. M. Polyansky, and A. P. Shergin, VII ICPEAC, Abstr. of papers, Amsterdam, The Netherlands, 1971, p. 397.

[11]E. Everhart, G. Stone, and R. J. Carbone, Phys. Rev. **99,** 1287 (1955).

[12]V. K. Nikulin, Zh. Tekh. Fiz. **41,** 33 (1971) [Sov. Phys. Tech. Phys. **16,** 21 (1971)].

[13]V. K. Nikulin, Zh. Tekh. Fiz. **41,** 41 (1971) [Sov. Phys. Tech. Phys. **16,** 28 (1971)].

[14]Landolt-Bornstein, Zahlenwerte und Funktionen, 1, Atom und Molekular Physik, Berlin, 1950.

[15]T. F., O'Malley, J. Chem. Phys. **51,** 322 (1969).

[16]V. Fano and W. Lichten, Phys. Rev. Lett. **14,** 627 (1965); W. Lichten, Phys. Rev. **164,** 131 (1967).

[17]O. B. Firsov, Zh. Eksp. Teor. Fiz. **24,** 279 (1953).

[18]R. P. Marchi, Phys. Rev. **183,** 185 (1969).

[19]V. V. Afrosimov, A Survey of Phenomena in Ionized Gases, Invited papers, Papers, Vienna, 1968, p. 91.

[20]T. A. Green and R. E. Johnson, Phys. Rev. **152,** 9 (1966).

[21]M. Matsuzawa, J. Phys. Soc. Jap. **25,** 1153 (1968).

[22]K. W. Ford and J. A. Wheeler, Ann. Phys. (N.Y.) **7,** 259 (1959); Ann. Phys. (N.Y.) **7,** 287 (1959).

[23]L. P. Kotova and M. Ya. Ovchinnikova, Zh. Eksp. Teor. Fiz. **60,** 2026 (1971) [Sov. Phys. JETP **33,** 1092 (1971)].

[24]E. E. Nikitin and M. Ya. Ovchinnikova, Usp. Fiz. Nauk **104,** 379 (1971) [Sov. Phys. Usp. **14,** 394 (1972)].

[25]D. Coffey, Jr., D. C. Lorents, and F. T. Smith, Phys. Rev. **187,** 201 (1969).

[26]J. Baudon, M. Barat, and M. Abignoli, J. Phys. B (1968–1969) **3,** 207 (1970).

[27]V. V. Afrosimov, Yu. S. Gordeev, V. M. Lavrov, and V. K. Nikulin, VII ICPEAC, Abstracts of papers, Amsterdam, The Netherlands, 1971, p. 143.

Translated by C. S. Robinson
102